Biochemical and Biophysical Research Communications **287,** 147–152 (2001)
doi:10.1006/bbrc.2001.5556, available online at http://www.idealibrary.com on IDEAL®

Pressure Denaturation of the Yeast Prion Protein Ure2

Jun-Mei Zhou,* Li Zhu,* Claude Balny,†,[1] and Sarah Perrett*

**National Laboratory of Biomacromolecules, Institute of Biophysics, Chinese Academy of Sciences, Beijing, China 100101; and †INSERM Unité 128, IFR 24, CNRS, 1919 route de Mende, 34293 Montpellier Cedex 5, France*

Received July 11, 2001

Denaturation of the *Saccharomyces cerevisiae* prion protein Ure2 was investigated using hydrostatic pressure. Pressures of up to 600 MPa caused only limited perturbation of the structure of the 40-kDa dimeric protein. However, nondenaturing concentrations of GdmCl in combination with high pressure resulted in complete unfolding of Ure2 as judged by intrinsic fluorescence. The free energy of unfolding measured by pressure denaturation or by GdmCl denaturation is the same, indicating that pressure does not induce dimer dissociation or population of intermediates in 2 M GdmCl. Pressure-induced changes in 5 M GdmCl suggest residual structure in the denatured state. Cold denaturation under pressure at 200 MPa showed that unfolding begins below −5°C and Ure2 is more susceptible to cold denaturation at low ionic strength. Results obtained using two related protein constructs, which lack all or part of the N-terminal prion domain, were very similar.

Key Words: **Ure2p; amyloid; guanidinium chloride; center of spectral mass; protein stability; protein folding; dimer.**

Ure2 is a 40-kDa homodimeric protein (1, 2) involved in regulation of nitrogen metabolism in the yeast *Saccharomyces cerevisiae* (3, 4). An interesting aspect of Ure2 function *in vivo* is its ability to propagate a heritable phenotype at the protein level by undergoing a structural change into an aggregated form (5, 6). Ure2 is thus termed a yeast prion (5), by analogy to the mammalian prion diseases (7). The Ure2 protein consists of two structural regions with distinct functions. The Asp/Glu rich, poorly structured N-terminal region (2, 8) is required for prion function *in vivo* (6) and amyloid formation *in vitro* (1). The globular C-terminal nitrogen regulatory domain (2, 8), for which the crystal structure has been solved (9, 10), shows homology to glutathione *S*-transferases (GST), a family of enzymes involved in cellular detoxification (4). Studies using GdmCl as a denaturant show that removal of all or part of the N-terminal prion domain has no affect on the thermodynamic stability, oligomeric state, kinetics of folding or folding pathway of Ure2 (2, 11). Ure2 cannot be fully denatured in urea and thermal denaturation is not reversible (2). Ure2 displays a tendency to aggregate or misfold, irrespective of the presence of the N-terminal domain (2, 11, 12). In prion strains, Ure2 protein is present in the cell as distinctive aggregates (13). A pH-induced increase in aggregation *in vitro* correlates with an increased tendency to form amyloid (12). *In vitro* seeding with preformed Ure2 amyloid fibrils is observed to increase both amyloid formation and aggregation (14). This suggests that while aggregation is principally a property of the globular C-terminal region, a relationship between formation of aggregated, amyloid, and prion forms of Ure2 nevertheless exists.

At the present time, protein folding is an extremely active field of research, lying at the interface between the biological and physical sciences. The use of high pressure has been shown to be a powerful tool in the study of the folding and dissociation of oligomeric proteins (15–17). The fundamental principles derived from *in vitro* folding experiments have practical application in understanding the pathology of diseases of protein misfolding, such as the amyloid diseases (18, 19). The generic cross-β fibrillar quaternary structure of amyloid fibrils appears to be independent of the particular disease or protein precursor (20). The diversity of proteins involved in amyloid diseases implies that amyloid formation requires significant structural change in the precursor protein. Like the yeast prion proteins (21), the mammalian prion protein PrP is found in a radically different structural form in diseased individuals (7). Understanding the structural and folding behavior of the prion proteins therefore represents a crucial first step toward understanding the molecular mechanism of prion propagation.

Abbreviations used: 90Ure2, Ure2 variant which lacks the N-terminal prion domain (residues 1–89); Δ15–42Ure2, Ure2 variant in which residues 15–42 have been deleted; CSM, center of spectral mass; EG, ethylene glycol; GdmCl, guanidinium hydrochloride.

[1] To whom correspondence and reprint requests should be addressed. Fax: 33 4 67 52 36 81. E-mail: balny@crbm.cnrs-mop.fr.

0006-291X/01 $35.00

Here we use hydrostatic pressure as a denaturing agent to investigate further the physical properties of the yeast prion protein Ure2. Under the conditions used (pH 8.4, 25°C, and 1 μM protein concentration) Ure2 folding is reversible (2). As well as full length Ure2, we examine two closely related proteins: 90Ure2 which lacks residues 1–89 and hence lacks the N-terminal prion domain as defined by biological activity (6, 21) or inspection of the sequence (2); and Δ15–42Ure2, which lacks residues 15–42, which is the island of "normal" amino acid sequence within the prion domain (2). These three proteins have been shown to have identical oligomeric structure and to show identical thermodynamic stability and kinetics of folding by GdmCl denaturation (2, 11).

MATERIALS AND METHODS

Preparation of yeast Ure2 constructs. Ure2, Δ15–42Ure2 and 90Ure2, containing a short N-terminal histidine tag, were produced from a synthetic gene in *Escherichia coli* as described previously (2). His-tagged Ure2 has normal biological activity *in vivo* (22), amyloid forming ability *in vitro* (1) and the same oligomeric structure, stability and equilibrium folding behavior as untagged protein (2). The experimental conditions used throughout were Tris–HCl, pH 8.4, 0.2 M NaCl, 25°C, and 1 μM protein concentration unless otherwise stated.

Fluorescence measurements. Fluorescence measurements were carried out using an Aminco Bowman Series 2 (AB2) fluorospectrophotometer in which the sample house was modified in the INSERM laboratory to allow measurement of fluorescence at pressures between 2 and 600 MPa using a thermostated pressure bomb. The fluorescence spectra were quantified by calculating the center of spectral mass (CSM), $\langle \nu \rangle$, as described by Weber and co-workers (23, 24):

$$\langle \nu \rangle = \Sigma \nu_i \times F_i / \Sigma F_i,$$

where ν_i is the wavenumber and F_i the fluorescence intensity at ν_i. The CSM is an intensity-weighted average emission wavenumber and detects changes in the environment of aromatic residues which reflects variations in the protein structure. The excitation wavelength for the intrinsic fluorescence was 280 nm (8-nm slit width) and the emission was recorded between 300 and 400 nm (8-nm slit width, 1-nm step size). The free energy and standard volume change upon unfolding, ΔG_0 and ΔV, were calculated as described (25).

Comparison of a large number of denaturation curves measured at atmospheric pressure for the three proteins studied here showed variation in the folded and unfolded CSM values between experiments which showed no correlation with the individual proteins (not shown). This is apparently an inherent characteristic of the protein and may be due to the presence of a small degree of aggregation, induced by factors that are not yet fully understood. In contrast, the observed change in CSM on denaturation, expressed as the change in emission maximum ($\Delta\lambda$), was highly reproducible between experiments and between proteins. Therefore, for the purposes of this study, variations in $\Delta\lambda$ are considered to be important, whereas variations in the initial and final CSM values are not considered significant. For the experiments presented here, the same batch of protein, treated in an identical manner, was used for all experiments, allowing the susceptibility of each protein to different methods of structural perturbation to be compared.

Cold denaturation. For cold denaturation experiments, the sample was first pressurized to 200 MPa at 25°C and then the temperature was decreased stepwise to −20°C. Under these conditions, according to the phase diagram of water, the sample solution stays in the liquid state if the pressure is maintained at 200 MPa. Water condensation and ice formation on the sapphire windows were avoided by directing a fine dry nitrogen gas flow over the windows.

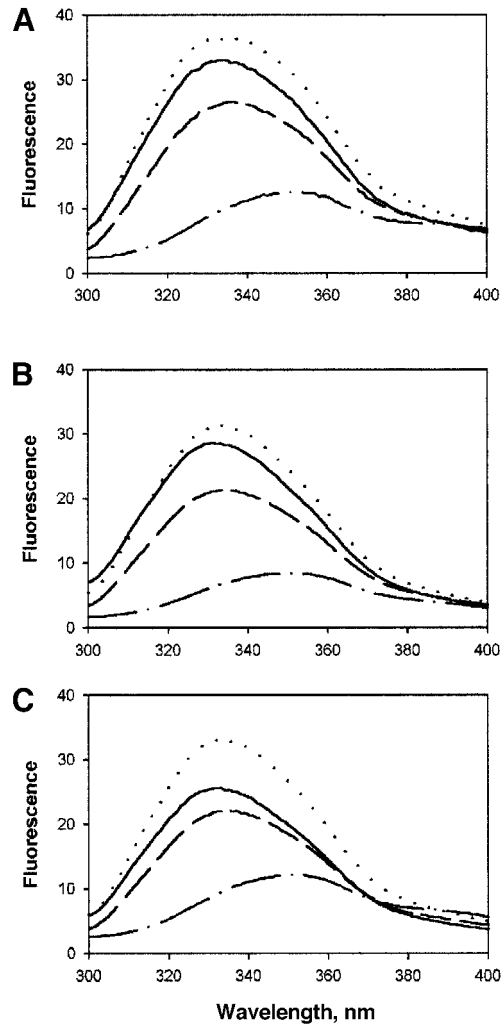

FIG. 1. Effect of high pressure on the fluorescence intensity of the emission spectra of (A) Ure2, (B) Δ15–42Ure2, and (C) 90Ure2 in 50 mM Tris–HCl, pH 8.4, containing 0.2 M NaCl at 25°C using 1 μM protein. The excitation wavelength was 280 nm. Symbols: low pressure (2–3 MPa), solid line; moderate pressure (200 MPa), dotted line; high pressure (500–600 MPa), dashed line; high pressure plus 2 M GdmCl, dashed–dotted line.

RESULTS AND DISCUSSION

Pressure Denaturation of Ure2

The effects of pressurization on the intrinsic fluorescence of Ure2 and its two N-terminally truncated mutants, Δ15–42Ure2 and 90Ure2, were measured using intrinsic fluorescence as a structural probe. The emission spectra of the three constructs are shown in Fig. 1. As the pressure was increased from 2–3 to 200 MPa, a gradual increase in the emission intensity was ob-

TABLE 1

Thermodynamic Parameters for Pressure-Induced Unfolding of Ure2 in the Presence of Different Concentrations of GdmCl at pH 8.4 and 25°C[a]

[GdmCl] (M)	Parameter	Ure2	Δ15-42Ure2	90Ure2	ΔG_{D-N}[c]
0	ΔV	−28 (±2)	−25 (±2)	[b]	
	ΔG_0	−5.6 (±0.4)	−5.6 (±0.6)	[b]	−52 (±2)
	Δλ	2.3	2.5	2.4	
1	ΔV	−33 (±3)	−50 (±7)	−32 (±2)	
	ΔG_0	−11 (±1)	−16 (±2)	−10.8 (±0.4)	−34 (±2)
	Δλ	8.2	7.0	6.3	
2	ΔV	−78 (±6)	−64 (±6)	−100 (±10)	
	ΔG_0	−19 (±2)	−16 (±2)	−24 (±3)	−17 (±3)
	Δλ	11.0	10.4	10.7	
3	ΔV	−47 (±5)	nd	nd	
	ΔG_0	−7 (±1)	nd	nd	0 (±3)
	Δλ	8.3	nd	nd	
5	ΔV	nd	−22 (±4)	nd	
	ΔG_0	nd	−6 (±1)	nd	36 (±5)
	Δλ	nd	2.0	nd	

[a] ΔV, the volume change in mL.mol^{-1}; ΔG_0, the free energy of unfolding in kJ.mol^{-1}, extrapolated to atmospheric pressure in the GdmCl concentration shown; Δλ, the shift in the emission maximum in nanometers, due to the pressure change from 2 to 600 MPa, taken directly from the experimental data and therefore independent of the fit; nd, not determined. Standard errors for the fit are shown in parentheses.

[b] The data could not be fit to a sigmoidal curve.

[c] ΔG_{D-N}, the free energy of unfolding in the concentration of GdmCl shown in kJ.mol^{-1}, calculated from the previously published GdmCl denaturation data (2) according to the equation $\Delta G_{D-N} = \Delta G_{H_2O}$, D–N − m[GdmCl]. The m value is 18 (±1) kJ.mol^{-1} M^{-1} (2).

served. On further increasing the pressure from 200 to 600 MPa, the emission intensity gradually decreased. With increasing pressure, a slight red shift in the emission maximum (Δλ) was observed (Fig. 1 and Table 1). The red shift is apparent as a linear or slightly sigmoidal decrease in the center of spectral mass with increasing pressure (Fig. 2) and accounts for around 20% of the change expected on complete unfolding of the protein (Table 1). This indicates that aromatic residues become more exposed to solvent due to the effects of pressure on the folded structure of Ure2. However, it is clear that hydrostatic pressure, even as high as 600 MPa, cannot induce complete unfolding of Ure2, or of Ure2 variants that lack all or part of the prion domain.

A previous study showed that creatine kinase (CK), a dimeric protein of similar size and stability to Ure2, is also relatively resistant to pressure unfolding (26). The application of high pressure caused CK to adopt a partially folded intermediate state, closely resembling the molten globule state populated in moderate concentrations of GdmCl (27). Under the conditions of pH and temperature used in these experiments, no intermediates are populated during the equilibrium denaturation of Ure2 (2). Two kinetic intermediates are populated during refolding of Ure2 under these conditions, including an on-pathway dimeric intermediate (11). This dimeric intermediate is apparently stabilized at lower pH (12). Folding intermediates are believed to have a role in prion and amyloid formation (11, 12). The slight structural change indicated by the shift in emission maximum and free energy change (Table 1) could indicate that the Ure2 pressure induced state is a native-like intermediate. Alternatively, the change could be due to unfolding of a fraction of the protein molecules.

Unfolding of Ure2 by a Combination of High Pressure and GdmCl

As hydrostatic pressure alone was insufficient to induce complete unfolding of Ure2, we investigated the effect of adding the chemical denaturant GdmCl (26). At atmospheric pressure, Ure2 is fully folded in 2 M GdmCl, fully denatured in 5 M GdmCl and the midpoint for the unfolding transition is 3 M GdmCl, as judged by a range of structural probes (2). The combination of 1 M GdmCl and hydrostatic pressure of up to 600 MPa is sufficient to unfold only a proportion of Ure2 molecules (Fig. 2 and Table 1). When 2 M GdmCl is combined with high pressure, the protein fluorescence spectrum shows a marked decrease in emission intensity (Fig. 1) and a red shift in the emission maximum (Δλ) of around 11 nm (Figs. 1 and 2; Table 1) as is observed on denaturation in 5 M GdmCl (2). This therefore defines conditions where a pressure jump could be used to measure kinetics of unfolding of Ure2. The thermodynamic parameters for pressure induced unfolding of Ure2 constructs in the presence of different concentrations of GdmCl are shown in Table 1.

The midpoint of pressure unfolding in 2 M GdmCl is the same within error for the three Ure2 constructs at around 250 MPa. The mean free energy of unfolding in

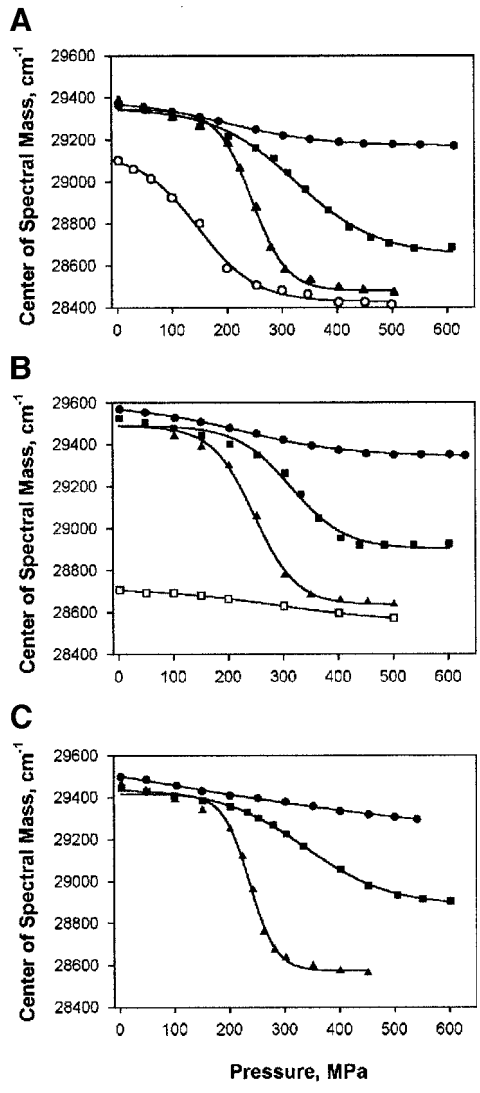

FIG. 2. Pressure dependence of the center of spectral mass of (A) Ure2, (B) Δ15–42Ure2, and (C) 90Ure2 in the presence of different concentrations of GdmCl. Symbols: 0 M GdmCl (filled circles), 1.0 M GdmCl (filled squares), 2.0 M GdmCl (triangles), 3.0 M GdmCl (open circles), and 5.0 M GdmCl (open squares). Other details are as in Fig. 1.

2 M GdmCl extrapolated to atmospheric pressure is 20 (±3) kJ.mol^{-1}. The free energy of unfolding measured by GdmCl denaturation is likewise the same within error for these three proteins and corresponds to a value under the same experimental conditions of 17 (±3) kJ.mol^{-1} (Table 1). This is consistent with the finding that there is no discernable effect of the prion domain on the stability or folding of Ure2 over a wide range of conditions (2, 11, 12). This also indicates that pressure induced unfolding in the presence of nondenaturing concentrations of GdmCl occurs by the same mechanism as GdmCl denaturation.

At pH 8.4 and 25°C, the GdmCl induced equilibrium denaturation transition is two-state and shows no protein concentration dependence (2). Cross-linking experiments show that dimeric structure persists after no further structural changes are detected by fluorescence or far-UV CD (L.Z., J.M.Z., and S.P., unpublished results). This means that the transition observed for GdmCl denaturation corresponds to unfolding, with dissociation occurring silently within the unfolded baseline region. This therefore indicates that unlike many oligomeric proteins (15, 26, 28, 29), high pressure does not induce dissociation of the Ure2 dimer, nor does it induce population of partially-folded intermediates under these experimental conditions. This study suggests that other methods that cause marginal destabilization of Ure2, such as urea (2) or pH (12), could be combined with hydrostatic pressure and thus might provide a useful means of investigating partially folded intermediates of Ure2.

The observation of slight, pressure-induced structural changes in the presence of 5 M GdmCl (Fig. 2B and Table 1) suggests that the combination of high pressure and high GdmCl results in a more fully denatured state. A similar effect is observed in 3 M GdmCl (Fig. 2A and Table 1). This is consistent with other studies, which suggest residual structure in the denatured state of Ure2 (11).

Cold Denaturation

Cold denaturation of proteins can be measured at temperatures below the freezing point of water by the addition of anti-freeze agents, such as ethylene glycol (EG). Measurements at −20°C require addition of approximately 30% EG, but addition of even 10% EG to solutions of Ure2 causes significant aggregation (L.Z., S.P., and J.M.Z., unpublished results). The application of 200 MPa, allows measurement at temperatures down to −20°C in aqueous solution without the addition of antifreeze reagents (30–32).

The application of 200 MPa of pressure causes a slight change in the CSM of Ure2, as described above. Differences in the absolute CSM values for the three proteins in the curves displayed (Fig. 3) reflects normal variation between experiments and is not significant (see Materials and Methods). Between 0 and 25°C no significant change in protein conformation was observed. Below −5°C all three constructs begin to show a change in protein conformation. However, the total change in emission maximum between 25 and −20°C is only 1 nm for all three proteins, i.e., around 10% of that expected on full denaturation of the protein. Measurements could not be continued below −20°C due to the limitations of the experimental set-up. When the experiment was repeated at lower ionic strength (i.e., in 50 mM Tris buffer but without the addition of 200 mM NaCl), the observed change in emission maximum was 2.4 nm. This indicates that Ure2 is destabilized at subphysiological ionic strength. This also explains the

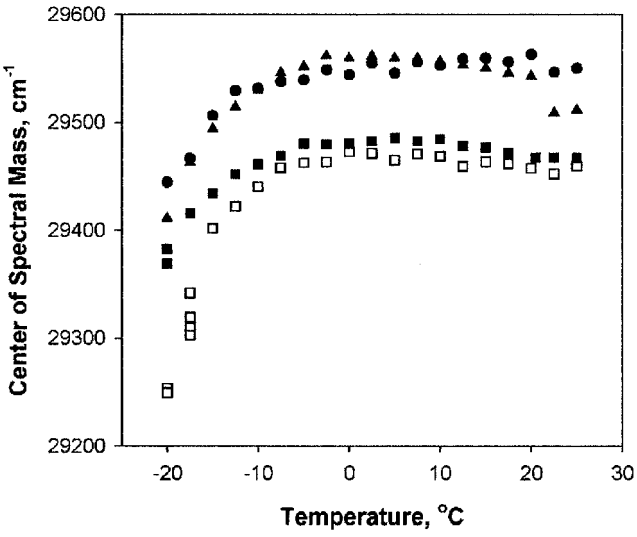

FIG. 3. Cold denaturation under 200 MPa of pressure of Ure2 (squares), Δ15–42Ure2 (triangles), and 90Ure2 (circles) in the presence (filled symbols) or absence (open symbols) of 0.2 M NaCl.

observation that less aggregation is observed on thawing when the protein is stored in buffer containing 0.2 M NaCl.

CONCLUSIONS

These data indicate that the N-terminal prion domain does not have any discernible effect on the global stability of Ure2, as was found previously (2). The application of high pressure or low temperature causes perturbation of the structure of Ure2, but without inducing global unfolding. Pressure induced unfolding in the presence of nondenaturing concentrations of GdmCl occurs by the same mechanism as GdmCl induced unfolding. This shows that high pressure does not induce dissociation of the Ure2 dimer and does not induce population of partially folded intermediates in 2 M GdmCl at pH 8.4.

ACKNOWLEDGMENTS

This work was supported by grants from INSERM/Chinese Academy of Sciences, the National Natural Science Foundation of China (30070163), and the 973 Project of the Chinese Ministry of Science and Technology (G1999075608). Initial stages of this work were supported by a grant from the BBSRC (to A. R. Fersht and S.P., University of Cambridge, UK). S.P. acknowledges support from the Royal Society, the Royal Commission for the Exhibition of 1851, and Sidney Sussex College (Cambridge, UK).

REFERENCES

1. Taylor, K. L., Cheng, N., Williams, R. W., Steven, A. C., and Wickner, R. B. (1999) Prion domain initiation of amyloid formation *in vitro* from native Ure2p. *Science* **283,** 1339–1342.
2. Perrett, S., Freeman, S. J., Butler, P. J. G., and Fersht, A. R. (1999) Equilibrium folding properties of the yeast prion protein determinant Ure2. *J. Mol. Biol.* **290,** 331–345.
3. Lacroute, F. (1971) Non-Mendelian mutation allowing ureidosuccinic acid uptake in yeast. *J. Bacteriol.* **106,** 519–522.
4. Coshigano, P. W., and Magasanik, B. (1991) The URE2 gene product of *Saccharomyces cerevisiae* plays an important role in the cellular response to the nitrogen source and has homology to glutathione *S*-transferases. *Mol. Cell. Biol.* **11,** 822–832.
5. Wickner, R. B. (1994) [URE3] as an altered URE2 protein: Evidence for a prion analog in *Saccharomyces cerevisiae. Science* **264,** 566–569.
6. Masison, D. C., and Wickner, R. B. (1995) Prion-inducing domain of yeast Ure2p and protease resistance of Ure2p in prion-containing cells. *Science* **270,** 93–95.
7. Prusiner, S. B. (1998) Prions. *Proc. Natl. Acad. Sci. USA* **95,** 13363–13383.
8. Thual, C., Komar, A. A., Bousset, L., Fernandez,-Bellot, E., Cullin, C., and Melki, R. (1999) Structural characterization of *Saccharomyces cerevisiae* prion-like protein Ure2. *J. Biol. Chem.* **274,** 13666.
9. Bousset, L., Belrhali, Janin, J., Melki, R., and Morera, S. (2001) Structure of the globular region of the prion protein Ure2 from the yeast *Saccharomyces cerevisiae. Structure (London)* **9,** 39–46.
10. Umlaud, T. C., Taylor, K. L., Rhee, S., Wickner, R. B., and Davies, D. R. (2001) The crystal structure of the nitrogen regulation fragment of the yeast prion protein Ure2p. *Proc. Natl. Acad. Sci. USA* **98,** 1459–1464.
11. Galani, D., Fersht, A. R., and Perrett, S. (2001) Folding of the yeast prion protein Ure2: Kinetic evidence for folding and unfolding intermediates. Submitted.
12. Thual, C., Bousset, L., Komar, A., Walter, S., Buchner, J., Cullin, C., and Melki, R. (2001) Stability, folding, dimerization, and assembly properties of the yeast prion Ure2p. *Biochemistry* **40,** 1764–1773.
13. Edskes, H. K., Gray, V. T., and Wickner, R. B. (1999) The [URE3] prion is an aggregated form of Ure2p that can be cured by overexpression of Ure2p fragments. *Proc. Natl. Acad. Sci. USA* **96,** 1498–1503.
14. Schlumpberger, M., Wille, H., Baldwin, M. A., Butler, D. A., Herskowitz, I., and Prusiner, S. B. (2000) The prion domain of yeast Ure2p induces autocatalytic formation of amyloid fibers by a recombinant fusion protein. *Protein Sci.* **9,** 440–451.
15. Silva, J. L., and Weber, G. (1993) Pressure stability of proteins. *Annu. Rev. Phys. Chem.* **44,** 89–113.
16. Gross, M., and Jaenike, R. (1994) Proteins under pressure. *Eur. J. Biochem.* **221,** 617–630.
17. Mozhaev, V. V., Heremans, K., Frank, J., Masson, P., and Balny, C. (1996) High pressure effects on protein structure and function. *Proteins* **24,** 81–91.
18. Kelly, J. W. (1997) Amyloid fibril formation and protein misassembly: A structural quest for insights into amyloid and prion diseases. *Structure (London)* **5,** 595–600.
19. Perrett, S. (1998) Misshapes and misfits: Protein misfolding and disease. *Chem. Ind. (London)* **10,** 389–393.
20. Blake, C., and Serpell, L. (1996) Synchrotron X-ray studies suggest that the core of the transthyretin amyloid fibril is a continuous beta-sheet helix. *Structure (London)* **5,** 595–600.
21. Wickner, R. B., Taylor, K. L., Edskes, H. K., Maddelein, M. L., Moriyama, H., and Roberts, B. T. (2000) Prions of yeast as heritable amyloidoses. *J. Struct. Biol.* **130,** 310–322.
22. Komar, A. A., Guillement, E., Reiss, C., and Cullin, C. (1998) Enhanced expression of the yeast Ure2 protein in *Escherichia*

coli: The effect of synonymous codon substitutions at a selected place in the gene. *Biol. Chem*. **379,** 1295–1300.

23. Silva, J. L., Miles, E. W., and Weber, G. (1986) Pressure dissociation and conformational drift of the beta dimer of tryptophan synthase. *Biochemistry* **25,** 5781–5786.
24. Ruan, K., and Weber, G. (1989) Hysteresis and conformational drift of pressure-dissociated glyceraldehyde phosphate dehydrogenase. *Biochemistry* **28,** 1279–1281.
25. Li, T., Hook, J., Drickamer, H. K., and Weber, G. (1976) Plurality of pressure-denatured forms in chymotrypsinogen and lysozyme. *Biochemistry* **15,** 5571–5580.
26. Zhou, J. M., Zhu, L., and Balny, C. (2000) Inactivation of creatine kinase by high pressure may precede dimer dissociation. *Eur. J. Biochem*. **267,** 1247–1253.
27. Fan, Y. X., Zhou, J. M., Kihara, H., and Tsou, C. L. (1998) Unfolding and refolding of dimeric creatine kinase equilibrium and kinetic studies. *Protein Sci*. **7,** 2631–2641.
28. Kornblatt, M. J., Lange, R., and Balny, C. (1998) Can monomers of yeast enolase have enzymatic activity? *Eur. J. Biochem*. **251,** 775–780.
29. Roitel, O., Bec, N., Lange, R., Balny, C., and Branlant, G. (2001) Pressure denaturation of phosphorylating glyceraldehyde-3-phosphate dehydrogenase from *Bacillus stearothermophilus*. *Biochem. Biophys. Res. Commun*. **283,** 347–350.
30. Zhang, J., Peng, X., Jonas, A., and Jonas, J. (1995) NMR study of the cold, heat, and pressure unfolding of ribonuclease A. *Biochemistry* **34,** 8631–8641.
31. Mombelli, E., Afshar, M., Fusi, P., Mariani, M., Tortora, P., Connelly, J., and Lange, R. (1997) The role of phe31 in maintaining the conformational stability of ribonuclease p2 from *Sulfolobus solfataricus* under extreme conditions of temperature and pressure. *Biochemistry* **36,** 8733–8742.
32. Dumoulin, M., Ueno, H., Hayashi, R., and Balny, C. (1999) Contribution of the carbohydrate moiety to conformational stability of the carboxypeptidase Y. *Eur. J. Biochem*. **262,** 475–483.